PHYSICAL REVIEW E **90**, 013006 (2014)

Finite time blow-up and breaking of solitary wind waves

M. A. Manna and P. Montalvo
Université Montpellier 2, Laboratoire Charles Coulomb UMR 5221, F-34095 Montpellier, France

R. A. Kraenkel
Instituto de Física Téorica, UNESP - Universidade Estadual Paulista, Rua Dr. Bento Teobaldo Ferraz 27, Bloco II, 01140-070 São Paulo, Brazil
(Received 20 March 2014; published 9 July 2014)

The evolution of surface water waves in finite depth under wind forcing is reduced to an antidissipative Korteweg–de Vries–Burgers equation. We exhibit its solitary wave solution. Antidissipation accelerates and increases the amplitude of the solitary wave and leads to blow-up and breaking. Blow-up occurs in finite time for infinitely large asymptotic space so it is a nonlinear, dispersive, and antidissipative equivalent of the linear instability which occurs for infinite time. Due to antidissipation two given arbitrary and adjacent planes of constant phases of the solitary wave acquire different velocities and accelerations inducing breaking. Soliton breaking occurs in finite space in a time prior to the blow-up. We show that the theoretical growth in amplitude and the time of breaking are both testable in an existing experimental facility.

DOI: 10.1103/PhysRevE.90.013006 PACS number(s): 47.35.Fg, 05.45.Yv, 47.35.Jk

Introduction. Experimental, theoretical, and numerical studies in the mechanisms of transfer of energy from wind to surface water waves are a classical matter of investigation in fluid dynamics. From a theoretical point of view the pioneering works are those of Jeffreys [1,2], Phillips [3], and Miles [4,5].

Jeffreys' theory supposes both the water as well as the air to be inviscid, incompressible, and obeying linearized equations of motion. The Jeffreys' theory allows us to compute the linear wave growth of wind-generated normal Fourier modes of wave number k. The physical mechanism behind this is *antidissipation*. Energy passes continuously from the air to the surface wave. Consequently the wave amplitude $\eta(x,t,k)$ (x space and t time) grows exponentially in time; i.e., $\eta(x,t,k) \sim \exp(\gamma_J t)$ more or less quickly according to the coefficient γ_J, which depends on the wind speed and the water depth h.

Once the linear and dispersionless approximation breaks down, nonlinear and dispersive processes begin to play a role. So the issue addressed here is, "How does one describe the evolution in time of a normal mode k, under the competing actions of (weak) nonlinearity, dispersion, and antidissipation?" Nonlinearity is likely to balance dispersive effects, or to stop exponential decay or growth of wave amplitude in time due to dissipation or antidissipation. Equilibrium between nonlinearity and dispersion can evolve in time to form solitary waves like in the Korteweg–de Vries equation [6,7]. Balance between dissipation or antidissipation and nonlinearity creates shock structures like in the Burgers equation [6].

The standard equation describing competition between weak nonlinearity, dispersion, and dissipation is the Korteweg–de Vries–Burgers (KdV-B) equation. It arises from many and various physical contexts (see Benney [8], Johnson [9], Grad and Hu [10], Hu [11], Wadati [12], and Karahara [13]). However in this work and in order to study simultaneous competing effects of nonlinearity, dispersion, and antidissipation we derive a KdV-B type equation with *dissipation turned into antidissipation*.

The antidiffusive KdV-B equation. Let us consider *a quasilinear* air-water system with the air dynamics linearized and the water dynamics considered nonlinear and irrotational. The system is $(2+1)$ dimensional (x,z,t) with x and z the vertical and the horizonal space coordinates. The aerodynamic air pressure $P_a(x,z,t)$ evaluated at the free surface $z=\eta(x,t)$ has a component in phase and a component in quadrature with the water elevation. For an energy flux to occur from the wind to the water waves there must be a phase shift between the fluctuating pressure and the interface. Hence, the energy transfer is only due to the component in quadrature with the water surface, or in other words in phase with the slope. To simplify the problem we consider, following Refs. [2,4,14], only the pressure component in phase with the slope on the interface; i.e.,

$$P_a = \epsilon\rho_a\Delta^2\eta_x \quad \text{with} \quad \Delta = [(\kappa U_1/\sqrt{C_{10}}) - c], \tag{1}$$

where $\epsilon < 1$ is the sheltering coefficient, $c = \sqrt{g/k}\tanh(kh)$, $U_1 = u_*/\kappa$ with u_* the friction velocity, $\kappa \sim 0.41$ the von Kármán constant, C_{10} the wind-stress coefficient, and g the gravitational acceleration. In order to adimensionalize the equations of motion we introduce dimensionless primed variables: $x = lx', z = hz', t = lt'/c_0, \eta = a\eta', \phi = gla\phi'/c_0, U_1 = c_0U_1'$ with ϕ the velocity potential and a and l typical wave amplitude and wavelength and $c_0 = \sqrt{gh}$. We define two dimensionless parameters $\nu = a/h < 1$ and $\delta = h/l < 1$. So with this assumption the complete irrotational Euler equations and boundary conditions are (dropping the primes)

$$\delta^2\phi_{xx} + \phi_{zz} = 0, \quad -1 \leqslant z \leqslant \nu\eta, \tag{2}$$

$$\phi_z = 0, \quad z = -1, \tag{3}$$

$$\eta_t + \nu\phi_x\eta_x - \frac{1}{\delta^2}\phi_z = 0, \quad z = \nu\eta, \tag{4}$$

$$\phi_t + \frac{\nu}{2}\phi_x^2 + \frac{\nu}{2\delta^2}\phi_z^2 + \eta + \delta\epsilon s\Delta^2\eta_x = 0, \quad z = \nu\eta, \tag{5}$$

where $s = \rho_a/\rho_w \sim 10^{-3}$ with ρ_a (ρ_w) the air (water) density. We solve the Laplace equation and its boundary conditions with an expansion in powers of $(z+1)$, $\phi = \sum_{m=0}^{m=\infty}(z+$

$1)^m\delta^m q_m(x,t)$. Substituting in Eq. (2) and using Eq. (3) we obtain $\phi = \sum_{m=0}^{m=\infty}(-1)^m \frac{(z+1)^{2m}}{(2m)!}\delta^{2m} q_{0,2mx}$. Using the kinematic and dynamics boundary conditions Eq. (4) and Eq. (5) and disregarding terms in $O(\nu\delta^2)$ and $O(\delta^4)$ we find, with $r = q_{0,x}$, the system

$$\eta_t + \{(1+\nu\eta)r\}_x - \tfrac{1}{6}\delta^2 r_{xxx} = 0, \tag{6}$$

$$\eta_x + r_t + \nu r r_x - \tfrac{1}{2}\delta^2 r_{xxt} + \delta\epsilon s\Delta^2\eta_{xx} = 0. \tag{7}$$

The linear wave solution of (6) and (7) moving to the right is $r(\xi) = \eta(\xi)$, $\xi = x - t$, with η (or r) an arbitrary function of ξ. Now we look for a solution with nonlinear corrections to the orders $O(\nu)$, $O(s\delta)$, and $O(\delta^2)$. Following the procedure in Whitham [6] we obtain

$$r = \eta - \frac{1}{4}\eta^2\nu + \frac{\epsilon}{2}\Delta^2\eta_x s\delta + \frac{1}{3}\eta_{xx}\delta^2 + O(\nu\delta^2, s^2\delta^2, \delta^4). \tag{8}$$

Substituting (8) in (6) and (7) we obtain an anti-dissipative KdV-B equation

$$\eta_t + \eta_x + \frac{3}{2}\nu\eta\eta_x + \frac{1}{6}\delta^2\eta_{xxx} + \frac{s}{2}\delta\epsilon\Delta^2\eta_{xx} = 0. \tag{9}$$

For traveling wave solutions, the action of dissipation or antidissipation in KdV-B is not of great matter except for the sign of the slope [15]. But soliton solutions under antidissipation exhibit a blow-up and breaking in finite time.

Blow-up and breaking of solitary waves in finite time. In the usual KdV-B equation the effect of (weak) dissipation through bottom friction for instance is to decrease slowly the amplitude and to increase slowly the width of the solitary wave solution, eventually flattening it in an infinite time. In our case antidiffusion increases the soliton amplitude and decreases the width of the solitary wave solution. Contrary to the diffusive KdV-B equation which dissipates energy in time, here the wave energy grows in time. Multiplying (9) by $\eta(x,t)$, assuming the limit $\eta(\pm\infty,t) = 0$, and integrating over all x we obtain $\frac{\partial}{\partial t}\int_{-\infty}^{\infty}\eta^2 dx = (s/4)\delta\epsilon\Delta^2\int_{-\infty}^{\infty}(\eta_x)^2 dx$. As the right-hand side is positive definite, the wave energy $E = \int_{-\infty}^{\infty}\eta^2 dx$ monotonically increases in time.

In KdV we must have balance between nonlinearity and dispersion; i.e., $O(\nu) \sim O(\delta^2)$. We assume the dissipative effects to be weaker than the dispersive and nonlinear ones, so we chose $(s/2)\delta\epsilon\Delta^2 \sim O(\delta^3)$. The validity of this hypothesis is checked by evaluating typical values of Δ for reasonable wind speeds, not higher than 20 m/s. With this scaling and after a Galilean transform in order to eliminate the term η_x, an approximate solution of Eq. (9) is given by (see Ref. [16] for the dissipative case)

$$\eta = a(t)\cosh^{-2}\left\{\alpha a(t)^{\frac{1}{2}}\left[x - t - \frac{\nu}{2}\int^t a(t')dt'\right]\right\}, \tag{10}$$

with $\alpha^2 = 3\nu/4\delta^2$ and $a(t)$ the time-dependent amplitude given by

$$a(t) = (1 - t/t_b)^{-1}, \tag{11}$$

where t_b is the *blow-up time* which can be explicated in terms of the system parameters as

$$t_b = 5\delta/(2s\epsilon\Delta^2\nu). \tag{12}$$

The phase $\theta(x,t)$ is local in x and t:

$$\theta(x,t) = \alpha\left(\frac{1}{1-\frac{t}{t_b}}\right)^{\frac{1}{2}}\left[x - t + \frac{\nu t_b}{2}\ln\left(1 - \frac{t}{t_b}\right)\right]. \tag{13}$$

As t approaches t_b, η goes to zero $\forall x$ except for x going to $+\infty$ as $\lim_{t\to t_b}[t - (\nu t_b/2)\ln(1 - t/t_b)]$. So at $x(t_b) \to +\infty$ the model presents an asymptotic, in space, *finite time blow-up*. This is a nonlinear, dispersive, and antidissipative instability analogous to the linear, antidissipative instability in the Jeffreys theory: the solitary wind wave replaces the sinusoidal wave and the blow-up for $x(t_b) \to +\infty$ in finite time $t = t_b$ replaces the local wave-amplitude divergence in infinite time.

For $t = t_b$ obviously the model breaks down. But well before blow-up the amplitude is such that the solitary wind wave breaks. Consequently before $t = t_b$ the model gives an accurate kinematic and dynamic description of the route towards breaking of solitary wind waves.

For large enough t, of course some nonlinear, dispersive, and dissipative higher-order effects will appear. However, our derived model (9) is of order 3 in δ; hence the longest allowed time τ has to be $\tau = \delta^3 t$, which is of order unity when t is large, such as $t_b \propto \delta^{-3}$. Hence, in order to keep the model valid, we checked that the derivatives of η in (9) stayed of order unity when $t < t_b$.

Wave-breaking criteria. The soliton blow-up being obviously impossible to probe experimentally, an interesting approach is to evaluate when the solitary wave breaks under this specific wind forcing, which will be before the blow-up. The breaking time t_d, and more generally breaking conditions, are subject to many discussions. A plethora of effective criteria exist in the literature to determine breaking. Hence, we studied three of the most widely known effective breaking criteria in order to compare t_d with t_b as given by (12). The first one is the *McCowan criterion* [17]. It is reached for a limiting ratio between the maximum wave height $a_{\max}$ and the water depth h given by $a_{\max}/h \approx 0.78$. The second is the *Miche criterion* [18]. It concerns the limiting wave slope a/λ. Breaking is reached for $(\frac{a}{\lambda})_{\max} = \frac{1}{7}\tanh(\frac{2\pi h}{\lambda})$. For the soliton solution λ is interpreted as an effective wavelength, and is time-dependent. In laboratory variables, it depends only on the wave height a and water depth h, as $\lambda = 2\pi\sqrt{\frac{4h^3}{3a}}$. Of course, a depends on time as of (11).

The third type of criterion we chose is *the wave horizontal velocity criterion* (*velocity criterion* for short); see Shemer [19] and references therein for instance. When the horizontal speed r exceeds the one of the phase plane at the crest, matter starts to be ejected from the wave, and breaking can occur. r is obtained from (8) and compared to the phase speed at the crest. This criterion depends directly on kinematics concerns, and is exempt from the empirical aspect of the two other laws. Hence, we have obtained the corresponding breaking time perturbatively for the velocity criterion and it reads

$$t_d = t_b\frac{5}{4}\nu + O(\nu^{3/2}). \tag{14}$$

Each criterion gives a different breaking time t_d, which is plotted in order to be compared to t_b. We took ranges of

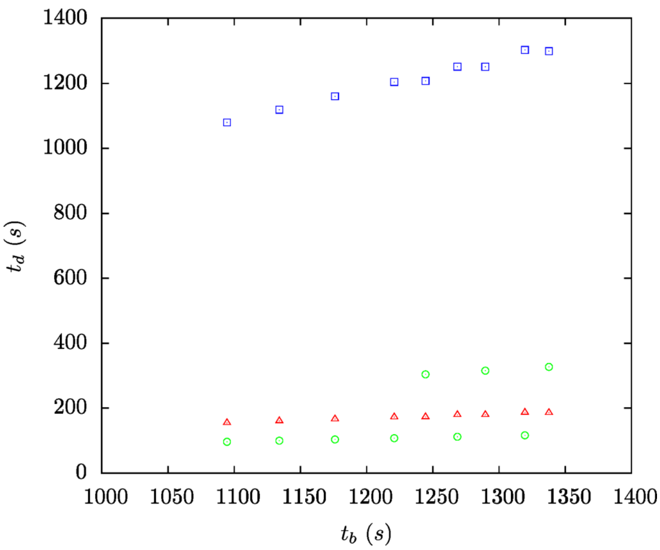

FIG. 1. (Color online) Comparison of velocity (red triangles), Miche (green circles), and McCowan (blue squares) criteria. Plotted are the trends for the allowed values of t_d, t_b for the parameter range, with $\nu = 1/10$. The breaking time, always inferior to the blow-up time, is extremely close to it in the case of the McCowan criterion. The Miche and velocity criteria yield breaking time values of similar order of magnitude.

parameter values such that $U_{10} \in [4;\ 22]$ m/s for the wind, and $h \in [0.1;\ 4]$ m. The results are shown in Fig. 1 and Fig. 2.

For $\nu = 1/10$ the McCowan criterion gives the highest values of t_d, the Miche criterion has a too big spread depending on the input parameters to be accurate, and we can see the velocity criterion yields the shortest time breaking values. In Fig. 2, we took a parameter value $\nu = \frac{1}{3}$. We checked that the orders in ν and δ in (9) were the same. But we cannot change the value of s, which is the air to water density ratio. In order to keep the balance between terms in (9), we have to consider higher Δ. This yields strong wind values up to $U_{10} \approx 20$ (m/s) at 10 m. In this framework, there is no drop of the drag coefficient [20], hence no foam formation, and the derived KdV-B equation is still valid. In this case the McCowan criterion gives lower values for the breaking time t_d and an even larger spread is obtained for the Miche criterion. We can see the velocity criterion gives values of t_d analogous to those in the $\nu = 1/10$ case. The kinematic criterion is more stable than the others with regards to parameter variations, and we consider it to be the most relevant for this study.

Kinematics description of wind solitary wave breaking. θ defines a local wave number $k = \partial\theta/\partial x$ and a local frequency $\omega = -\partial\theta/\partial t$, so the local phase velocity is

$$c(x,t) = \frac{\omega(x,t)}{k(x,t)} = 1 + \frac{\nu}{2}a(t) - \frac{\theta(x,t)a(t)^{\frac{1}{2}}}{2\alpha t_b}. \quad (15)$$

We also have a local phase acceleration

$$\gamma(x,t) = \frac{3\nu a(t)^2}{4t_b} + \frac{a(t)}{2t_b} - \frac{a(t)^{\frac{3}{2}}\theta(x,t)}{2\alpha t_b^2}. \quad (16)$$

The planes of constant phases $\theta(x,t) = \theta_0$ are moving with velocities $c(\theta_0,t)$ and accelerations $\gamma(\theta_0,t)$. In particular, two planes θ_1 and θ_2 around a given θ_0, i.e., $\theta_1 < \theta_0 < \theta_2$ (for example the soliton maximun) have speeds and accelerations such that $c(\theta_1,t) > c(\theta_2,t)$ and $\gamma(\theta_1,t) > \gamma(\theta_2,t)$. This kinematics disequilibrium of velocities and accelerations between two adjacent planes destroys the soliton symmetry and brings to the formation of a breaking for $t \to t_d$.

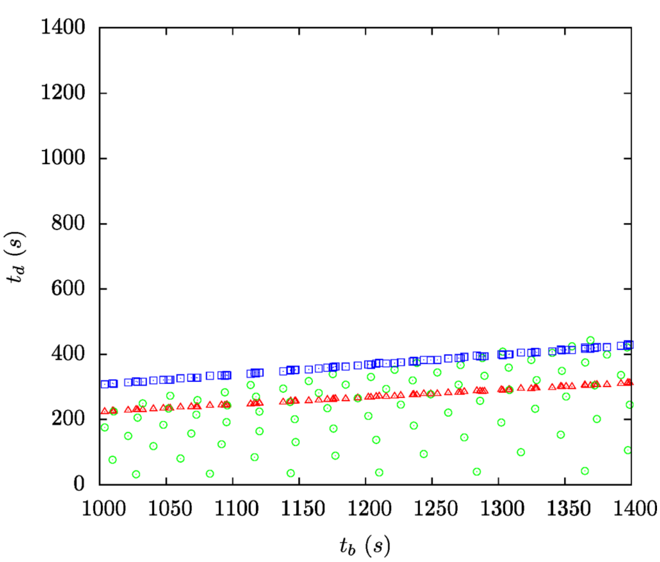

FIG. 2. (Color online) Same as in Fig. 1 with $\nu = 1/3$, with the wave velocity criterion in red triangles, Miche in green circles, and McCowan above, in blue squares. The higher amplitude yields shorter breaking times for McCowan and Miche, as well as a wider range of allowed values for the parameter range. There is a higher scatter in the Miche criterion values.

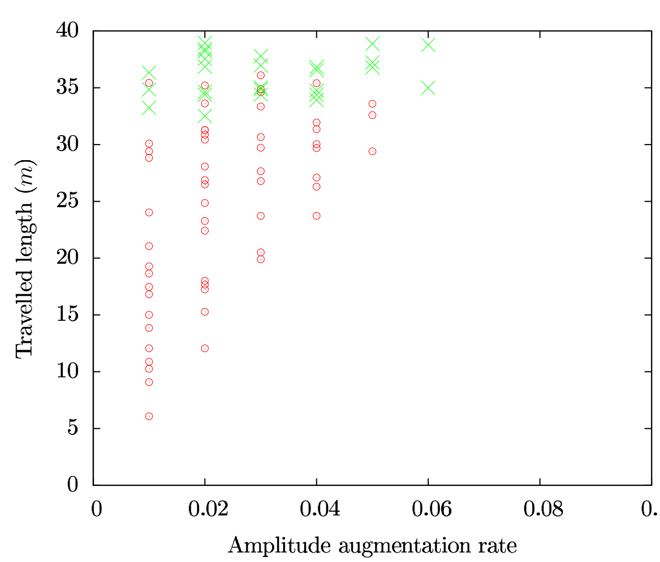

FIG. 3. (Color online) In a 40-m-long wind tunnel, this shows at what point and which time t a certain augmentation rate is attained. In red circles, we have $t < 10$ s, and on the upper part in green crosses we have $t \geqslant 10$ s. The values are computed for different constant depths between 0.7 and 1.0 m, a reference wind speed $U_{10} < 15$ m/s, and a wave steepness $ka > 0.23$. We see that with these conditions, the augmentation can be above 6%.

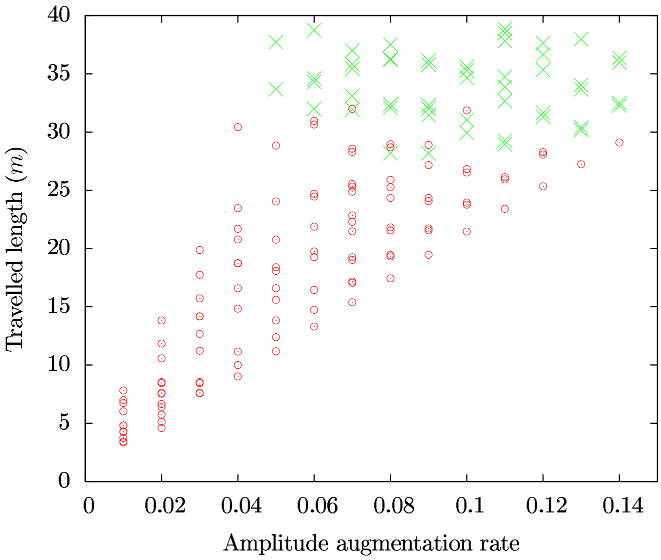

FIG. 4. (Color online) Same as in Fig. 3 with the ranges of wind and depth changed to 0.3 m $\leqslant h \leqslant$ 0.7 m, the reference wind speed 15 m/s $< U_{10} <$ 20 m/s, and the same wave steepness $ka > 0.23$. In red circles, $t <$ 10 s, in green crosses $t \geqslant$ 10 s. These conditions allow for a much greater energy transfer, hence a significantly faster growth. The amplitude increases by up to 15% within the tunnel length.

Prospect of an experimental test. In this last section we are going to show that the theoretical growth in amplitude and the time of breaking are both testable in the existing experimental facility.

The Jeffreys mechanism acts only on waves steep enough to shelter the front side from the wind. Typically, a steepness parameter such as $ka > 0.3$ is necessary (see Montalvo *et al.* [21,22] and references therein). However, at $t = 0$, we can see that (10) is too smooth to allow sheltering. In order to have a steep enough soliton, setting the ν parameter to $\frac{1}{3}$ is necessary. Now, with this set we define t_n the time taken by the maximum soliton amplitude to grow of $n\%$. We have then $t_n = \frac{n}{n+1} t_b$. We suppose that the soliton is created in a 40-m-long wind tunnel which can be filled up to 1 m of water depth. This configuration is close to the IRPHE wind tunnel in Luminy, France. It allows us then to evaluate what is the augmentation of the soliton in those given constraints. The results are shown in Figs. 3 and 4. These results show that, given this particular type of wind-wave tank, a fair augmentation of the soliton amplitude can be measured before the end of the tunnel is reached. This shows that our model can indeed be tested, as confronting the measured augmentation time with the theoretical one is possible.

Acknowledgments. The authors thank H. Branger from IRPHE Marseille for valuable discussion about experimental possibilities. P.M. thanks Labex NUMEV (Digital and Hardware Solutions, Modeling for the Environment and Life Sciences) for partial financial support. M.A.M. thanks the PVE program (Pesquisador Visitante Especial, CAPES/BRASIL). P.M. and M.A.M. acknowledge ANR Grant No. ANR-13-ASTR-0007 for partial financial support.

[1] H. Jeffreys, Proc. R. Soc. A **107**, 189 (1925).
[2] H. Jeffreys, Proc. R. Soc. A **110**, 241 (1926).
[3] O. Phillips, J. Fluid Mech. **2**, 417 (1957).
[4] J. Miles, J. Fluid Mech. **3**, 185 (1957).
[5] J. Miles, Appl. Mech. Rev. **50**, R5 (1997).
[6] G. Whitham, *Linear and Nonlinear Waves* (Wiley Interscience, New York, 1974).
[7] D. Korteweg and G. de Vries, Philos. Mag. **39**, 422 (1895).
[8] D. J. Benney, J. Math. Phys. **45**, 150 (1966).
[9] R. Johnson, Phys. Fluids **15**, 1693 (1972).
[10] H. Grad and P. Hu, Phys. Fluids **10**, 2596 (1967).
[11] P. Hu, Phys. Fluids **15**, 854 (1972).
[12] M. Wadati, J. Phys. Soc. Jpn. **38**, 673 (1975).
[13] T. Karahara, J. Phys. Soc. Jpn. **28**, 1321 (1970).
[14] C. Kharif, R. Kraenkel, M. Manna, and R. Thomas, J. Fluid Mech. **664**, 138 (2010).
[15] A. Jeffrey and S. Xu, Wave Motion **11**, 559 (1989).
[16] E. Ott and R. Sudan, Phys. Fluids **13**, 1432 (1970).
[17] J. McCowan, Philos. Mag. Series 5 **38**, 351 (1894).
[18] M. Miche, *Mouvement ondulatoires de la mer en profondeur constante où décroissante*, Annales des Ponts et Chaussées, Tome 114, Paris, 1944.
[19] L. Shemer, Nat. Hazards Earth Syst. Sci. **13**, 2101 (2013).
[20] V. Makin, Boundary Layer Meteorology **115**, 169 (2004).
[21] P. Montalvo, J. Dorignac, M. Manna, C. Kharif, and H. Branger, Coastal Engineering **77**, 49 (2013).
[22] P. Montalvo, R. Kraenkel, M. A. Manna, and C. Kharif, Nat. Hazards Earth Syst. Sci. **13**, 2805 (2013).